

Effects of functionalized silver nanoparticles on aggregation of human blood platelets

This article was published in the following Dove Press journal:
International Journal of Nanomedicine

Justyna Hajtuch¹
Nadhim Hante²
Ewelina Tomczyk³
Michał Wojcik³
Marek Witold Radomski⁴
Maria Jose Santos-Martinez²
Iwona Inkielewicz-Stepniak¹

¹Department of Medical Chemistry, Medical University of Gdansk, Gdansk, Poland; ²School of Pharmacy and Pharmaceutical Sciences, Trinity College Dublin, Dublin 2, Ireland; ³Faculty of Chemistry, University of Warsaw, Warsaw, Poland; ⁴Department of Anatomy, Physiology and Pharmacology, University of Saskatchewan, Saskatoon, Canada

Purpose: We studied the effects of silver nanoparticles (AgNPs) on human blood platelet function. We hypothesized that AgNPs, a known antimicrobial agent, can be used as blood-compatible, “ideal material” in medical devices or as a drug delivery system. Therefore, the aim of the current study was to investigate if functionalized AgNPs affect platelet function and platelets as well as endothelial cell viability in vitro.

Methods: AgNPs, functionalized with reduced glutathione (GSH), polyethylene glycol (PEG) and lipoic acid (LA) were synthesized. Quartz crystal microbalance with dissipation was used to measure the effect of AgNPs on platelet aggregation. Platelet aggregation was measured by changes in frequency and dissipation, and the presence of platelets on the sensor surface was confirmed and imaged by phase contrast microscopy. Flow cytometry was used to detect surface abundance of platelet receptors. Lactate dehydrogenase test was used to assess the potential cytotoxicity of AgNPs on human blood platelets, endothelial cells, and fibroblasts. Commercially available ELISA tests were used to measure the levels of thromboxane B₂ and metalloproteinases (MMP-1, MMP-2) released by platelets as markers of platelet activation.

Results: 2 nm AgNPs-GSH, 3.7 nm AgNPs-PEG both at 50 and 100 µg/mL, and 2.5 nm AgNPs-LA at 100 µg/mL reduced platelet aggregation, inhibited collagen-mediated increase in total P-selectin and GPIIb/IIIa, TXB₂ formation, MMP-1, and MMP-2 release. The tested AgNPs concentrations were not cytotoxic as they did not affect, platelet, endothelial cell, or fibroblast viability.

Conclusion: All tested functionalized AgNPs inhibited platelet aggregation at nontoxic concentrations. Therefore, functionalized AgNPs can be used as an antiplatelet agent or in design and manufacturing of blood-facing medical devices, such as vascular grafts, stents, heart valves, and catheters.

Keywords: functionalized silver nanoparticles, blood platelets, QCM-D, platelets receptors, TXB₂, MMP-1 and MMP-2

Correspondence: Maria Jose Santos-Martinez
School of Pharmacy and Pharmaceutical Sciences, Trinity College Dublin, Dublin 2, Ireland
Tel +353 1 896 4281
Fax +353 1 608 2821
Email santosmm@tcd.ie

Iwona Inkielewicz-Stepniak
Department of Medical Chemistry, Medical University of Gdansk, Debinki 1 St. Gdansk 80-211, Poland
Tel +48 58 349 1450
Fax +48 58 349 1450
Email iinkiel@gumed.edu.pl

Introduction

Among metal nanoparticles, silver nanoparticles (AgNPs) are emerging as an attractive tool for many nanomedical applications.¹ They are endowed with anticancer, antibacterial, antifungal, and antiviral properties.² They can also be used to design an “ideal material” for bone prostheses, reconstructive orthopedic surgery, cardiac devices, extracorporeal circulation, catheters, and surgical appliances.^{1,2} AgNPs have also potential to form a drug delivery platform.³ For any blood-facing applications of AgNPs, blood and platelet biocompatibility are an essential characteristic.

Therefore, a number of research groups studied the effects of AgNPs on platelet reactivity. However, these studies yielded controversial results and both platelet activator and inhibitory properties of AgNPs have been claimed.^{4–10}

Others and we have indicated that the biocompatibility of nanoparticles with components of the circulation system depends on their functionalization and physicochemical properties.^{4,10–12}

Conjugating nanoparticles and other nanomaterials with polyethylene glycol (PEG), known as PEGylation, is used widely as it offers a number of advantages. For example, PEGylated nanomaterials when used in protein delivery systems show increased protein solubility and stability, reduced immunogenicity, decreased clearance by the reticuloendothelial system, and increased plasma half-life leading to less frequent dosing.¹³ It has been found by our team, that conjugation of gold nanoparticles with PEG protects platelets from activation.⁴ Niidome et al, 2006 demonstrated that PEG modification of gold nanorods also reduced their in vitro toxicity.¹⁴ Moreover, we noticed that AgNPs coated with PEG, and lipoic acid (LA) decreased cytotoxicity against human cells compared to non-functionalized AgNPs and improved antibacterial, and antibiofilm activity.^{8,13,15,16}

Based on our previous observations, we have synthesized AgNPs functionalized with PEG, LA, and reduced glutathione (GSH) and evaluate their effect on platelet aggregation under flow to mimic conditions encountered in microvasculature in vivo. We also evaluated the safety potential of thus synthesized AgNPs in regards to cytotoxicity. Finally, we focused on molecular mechanisms of platelet-AgNPs interactions including determination of surface abundance of platelet receptors, thromboxane B₂ formation, and release of MMP-2, MMP-9 from collagen-stimulated platelets.

Materials and methods

Synthesis and characterization of AgNPs

Glutathione stabilized silver nanoparticles (AgNPs-GSH)

Five hundred mg (2.7 mmol) of silver nitrate was dissolved in 320 mL of water and reaction mixture was placed in water/ice bath in dark. Then, 1.96 g (6.38 mmol) of reduced GSH was added slowly in small portions. After that, a white, flocculant appeared as precipitate. Reaction mixture was stirred further 1.5 hrs and next 9 mL of saturated solution of sodium bicarbonate was added dropwise, which increased pH to 4.5 and resulted in the disappearance of precipitate.

Next, 1.21 g (31.9 mmol) of sodium borohydride dissolved in 80 mL of water was added rapidly to vigorously stirring reaction mixture. After 15 mins, color of reaction

mixture has changed to dark-brown. The resulting reaction mixture was stirred overnight at room temperature. After 12 hrs, the excess of unbounded GSH and aggregates formed during the synthesis of nanoparticles were precipitated by the addition 300 mL of isopropanol. The precipitate, thus formed, was centrifuged (10 mins, 5000 g, 0°C) and then nanoparticles were dissolved in 20 mL of water. Additionally, the above-described procedure of precipitation/centrifugation was repeated two times. Then, nanoparticles were put in SnakeSkin (3500-MW cut off) tube and dialyzed against distilled water for 3 days (water was changed every day).

Lipoic acid-stabilized silver nanoparticles (AgNPs-LA)

Briefly, 1.9 (9.2 mmol) g of LA and 700 mg (18.5 mmol) of sodium borohydride were dissolved in 1400 mL of water. Next, 70 mL of 25 mM silver nitrate and additional portion 1 g (26.43 mmol) of sodium borohydride in 200 mL of water in 200 mL of water were added and the resulting reaction mixture was stirred in dark for 5 hrs. Then, 300 mL of the mixture was placed in SnakeSkin (3500-MW cut off) tube and dialyzed against distilled water for 3 days (water was changed every day).

Polyethylene glycol-stabilized silver nanoparticles (AgNPs-PEG2000)

Polyethylene glycol (PEG, average molecular mass – 2000 Da) coated spherical silver nanoparticles were obtained as described by Chen and Wang and Vander Linden et al, with some modifications.^{17,18} Briefly, dodecylamine (0.75 g, 4.04 mmol) was dissolved in cyclohexane (25 mL) and 6 mL of 37% aqueous formaldehyde solution was added. After 15 mins of vigorous stirring, a cyclohexane phase was separated by centrifugation and washed two times with water (2×10 mL). Next, an aqueous silver nitrate (0.2 g AgNO₃, 1.17 mmol, dissolved in 10 mL of water) was added under vigorous stirring and the organic phase was separated after 40 mins by centrifugation at 5000 g for 10 mins.

To the hexane solution of nanoparticles, 55 mg (0.0275 mmol) of PEG-2000 Da dissolved in 3 mL of DCM was added and the reaction mixture was stirred for 1 h. The precipitate of PEG 2000 Da coated nanoparticles was collected by centrifugation (10 mins, 5000 g), washed and then dissolved in 10 mL of deionized water. To remove the excess of unbonded thiol a dialysis (10,000-MW cut off) process in deionized water was applied for 3 days (water was changed every day).

The synthesized nanoparticles were covered with dodecyloamine molecules. To introduce PEG molecules onto nanoparticles surface ligand-exchange reaction was performed. The reaction relies on adding excess of thiol (which have stronger affinity to nanoparticles than amines), so PEG molecules replace all dodecyloamine molecules on NPs surface. Then, after purification of nanoparticles from excess of unbounded molecules by dialysis, the successful exchange reaction was confirmed by a series of HNMR, transmission electron microscopy (TEM), small-angle X-ray diffraction (SAXRD) measurements. To evidence that only PEG molecules are present on NPs surface, we performed additional thermogravimetry analysis (TGA) measurements.

Characterization of nanoparticles

To characterize particle size, surface coverage and purity of the obtained nanoparticles a series of TEM, SAXRD, TGA, and Fourier Transform Infrared Spectroscopy (FTIR) measurements were performed. FTIR and TGA were carried out to confirm the success of the ligand-exchange reactions and to calculate the number of molecules attached to the nanoparticle's surface measurements. Distribution of AgNPs size was determined and measured based on TEM images using ImageJ software (JEM-1200 EX II TEM ((JEOL, Tokyo, Japan)) which allow us to determine diameters of NPs in TEM image. According to those data, we prepared histograms of size distribution.

Blood collection and platelet isolation

Following informed consent, blood was withdrawn from healthy volunteers who had not been on any medication known to interfere with platelet function for at least 2 weeks prior to the study. Written informed consent was obtained from the volunteers in accordance with the Declaration of Helsinki. Whole blood was collected and carefully mixed with 3.15% sodium citrate (9:1). Platelet-rich plasma (PRP) and washed platelet (WP) suspensions were prepared from blood as described by Radomski and Moncada, using phosphate buffer solution at the final concentration of 250,000 platelets/ μ L. PRP was also separated from heparinized whole blood (250 g, 20 mins) for MMP-2 ELISA assay.¹⁹

Platelet-poor plasma (PPP), which served as a blank, was obtained by centrifugation of PRP at 1500 g for 10 mins. Approval for this study was obtained from the School of Pharmacy and Pharmaceutical Sciences Trinity College Dublin Research Ethics Committee (2016-03-01 [R8]).

Cell culture and exposure to AgNPs

Human umbilical vein endothelial cells (HUVEC) and human gingival fibroblast culture (HGF-1) cell line were obtained from the American Type Culture Collection (ATCC CRL-1730™ and ATCC CRL-2014™, respectively) and maintained as a monolayer culture in T-75 cm² tissue culture flasks. HUVEC were cultured in Ham's F12K medium adjusted to contain 2 mM L-glutamine, 1.5 g/L sodium bicarbonate, 0.1 mg/mL heparin, 0.03 mg/mL endothelial cell growth supplement, and 10% fetal bovine serum. HGF-1 cells were grown in Dulbecco's Modified Eagle's Medium (Sigma Aldrich), a high glucose medium (4.5 g/L) containing sodium pyruvate (110 mg/L), and supplemented with 10% fetal bovine serum, 6 μ g/mL penicillin-G, and 10 μ g/mL streptomycin. Cells were cultured at 37°C in a humidified atmosphere of 95% O₂, 5% CO₂. When confluent, cells were detached enzymatically with trypsin-EDTA and sub-cultured into a new cell culture flask. The medium was replaced every 2nd day.

For experiments, the cells were seeded in 96-well plates at a density of 2×10^4 cells/mL and allowed to attach for 24 hrs, then treated with AgNPs suspended in appropriate serum-free cell culture medium for another 24 hrs. Before use, the suspensions of AgNPs were shaken for 1 min. Controls were supplied with an equivalent-volume of serum-free cell culture medium in the absence of AgNPs.

Platelet aggregation monitored by light aggregometry

To monitor platelet viability, the response of platelets to collagen (2 μ g/mL) in PRP or WP was tested using light aggregometry. Briefly, PRP or WP samples (2.5×10^8 cells/mL) were placed in a PAP 8 aggregometer (Bio/Data Corporation, Horsham, PA, USA) and incubated for 20 mins at 37°C, with stirring at 900 r.p.m. in the presence or absence of collagen (2 μ g/mL).

Platelet aggregation measured by quartz crystal microbalance with dissipation (QCM-D)

The effect of AgNPs on platelet aggregation was measured using the Q-Sense® E4 QCM-D system (Q-Sense AB, Vastra Frolunda, Sweden) under flow conditions using a peristaltic microflow system (ISM 935; Ismatec SA, Glattbrugg, Switzerland) as previously described by our group. The working principle of QCM-D relies on the changes in resonance frequency f and energy dissipation D when an

alternating current is applied through a quartz crystal and material is adsorbed on the sensor surface. The deposition of mass on the crystal induces a negative f shift from the fundamental resonant frequency of the crystal (Δf) and a positive energy dissipation shift (ΔD) that allows the measurement of the formation of platelet-microaggregates at real time on the quartz surface interface.^{20,21}

For carrying out those experiments, polystyrene-coated quartz crystals with a frequency of 4.95 MHz were used as sensors following coating with fibrinogen. For fibrinogen coating, sensors were placed in fibrinogen dissolved in phosphate buffer solution (100 $\mu\text{g/mL}$) for 20 mins at room temperature. Fibrinogen-coated PC quartz crystals were then mounted in the flow chamber and perfused with PBS to ensure that fibrinogen loosely bound to the sensor was removed. Afterward, PRP suspensions were perfused through the device at 37°C at a flow rate of 100 $\mu\text{L/min}$ in the presence of vehicle or AgNPs (50 and 100 $\mu\text{g/mL}$). AgNPs-platelet's interactions were monitored for 20 mins in real time by the acquisition of Q-Sense software (QSoft401) and platelet aggregation measured and analyzed as changes in frequency (Δf) and dissipation (ΔD).

To study whether or not the interaction of AgNPs with plasma proteins could be responsible for the shifts in frequency and dissipation during the aggregation studies, the interaction of NPs with PPP was also investigated. For this purpose, PPP was perfused at 100 $\mu\text{L/min}$ in the presence and absence of NPs and Δf and ΔD were monitored also for 20 mins. Results from experiments using QCM-D are expressed as percentage of frequency and dissipation, where the maximal changes in frequency (negative shift) and dissipation (positive shift) at 20 mins of perfusion for the control (250,000 platelets/ μL) are considered as 100%.

Phase contrast microscopy

PRP suspensions were perfused in the presence of vehicle or AgNPs on fibrinogen-coated polystyrene-coated quartz crystals for 20 mins through the device. Next, crystal surfaces were observed by phase contrast microscopy an Axiovert 200M optical microscope (Carl Zeiss) using a 5 \times objective and photomicrographs were taken using a digital camera and AxioVision software (v 4.7; Carl Zeiss).

Lactate dehydrogenase (LDH) release assay

The cytotoxic effect of AgNPs was assessed by detecting LDH release following exposure of the WP at 37°C for 20 mins and 24 hrs, human cell line (HUVEC, HGF-1) for 24 hrs to 50 and/or 100 $\mu\text{g/mL}$ AgNPs using a Cytotoxicity Detection LDH kit

(Promega, Poland), according to the manufacturers' instructions. WP or cells treated with lysis buffer (0.1% Triton X-100) was used as a positive control (total LDH release). Lysis buffer-treated cells were set to 100%. AgNPs were used as background control and their absorbance were subtracted from the reading of the samples. Results are given as % of the total LDH release from the cells.

Flow cytometry

The abundance of P-selectin and PAC-1 on the surface of platelets in the presence of AgNPs (50 and/or 100 $\mu\text{g/mL}$) was detected by flow cytometry. Collagen (2 $\mu\text{g/mL}$) induced platelets aggregation in PRP was used as a positive control whereas PRP without collagen (resting platelets) was used as a negative control. Platelets in PRP were pre-incubated with AgNPs-GSH, AgNPs-PEG (50 and 100 $\mu\text{g/mL}$), or AgNPs-LA (100 $\mu\text{g/mL}$) for 5 mins prior to the addition of collagen (2 $\mu\text{g/mL}$). When collagen-induced aggregation reached 50% maximal light transmission, samples were collected and incubated in the dark for 5 or 15 mins at room temperature in the presence of 10 $\mu\text{g/mL}$ of P-selectin and GPIIb/IIIa (BD Biosciences, Oxford, UK), respectively. Subsequently, samples were diluted in FACSFlow™ and analyzed within 5 mins using a FACSArray™ bioanalyzer (BD Biosciences). Flow cytometry was performed on single-stained platelet samples as previously described.¹⁹ Platelets were identified by forward and side scatter signals, and 10,000 platelet-specific events were analyzed by the flow cytometer for fluorescence. Data were analyzed using FACSArray software (v 1.0.3; BD Biosciences) and expressed as a percentage of control fluorescence. AgNPs were not detected by the bioanalyzer.

TXB₂ formation

PRP (2.5×10^8 platelets/mL) was pre-incubated with AgNPs (50 and/or 100 $\mu\text{g/mL}$) for 5 mins and 2 $\mu\text{g/mL}$ collagen was added. Aggregation was halted when control reached maximum, by adding the equivalent-volume of 2 mM cold EDTA solution with 50 mM indomethacin. The samples were centrifuged at 12,000 $\times g$ for 10 mins at 4°C and the supernatant was collected and stored at -80°C. TXB₂, the stable metabolite of TXA₂, was measured using a TXB₂ enzyme immunoassay kit (Cayman Chemical, Ann Arbor, MI, USA), according to the instructions of the manufacturer. Absorbance values were also corrected with blank NPs.

MMP-1, MMP-2 release

Commercially available quantitative sandwiches ELISAs were used to measure concentrations of MMP-1 (total) (Abcam) and MMP-2 (both active and proactive) (R&D Systems, UK) released from platelets in PRP according to the manufacturer's protocol. Briefly, PRP (2.5×10^8 platelets/mL) was pre-incubated with AgNPs-GSH AgNPs-PEG, and AgNPs-LA (50 and/or 100 $\mu\text{g/mL}$) for 5 mins and 2 $\mu\text{g/mL}$ collagen was added and aggregation was halted after 20 mins, the samples were collected, centrifuged at $12,000 \times g$ for 10 mins at 4°C and the supernatant was stored at -80°C until analysis. The lower limits of detection were 8 $\mu\text{g/mL}$ for MMP-1 and 0.047 ng/mL for MMP-2.

Statistics

Data from at least three independent experiments were analyzed using GraphPad Prism (v 5.0; GraphPad Software, Inc, La Jolla, CA) and presented as means with standard deviation. Paired Student's *t*-tests, one-way

analyses of variance, and Tukey–Kramer post hoc multiple comparison test were performed, where appropriate. Statistical significance was considered when $p < 0.05$.

Results

Synthesis and characterization of functionalized AgNPs

We synthesized three types of functionalized AgNPs: AgNPs-GSH, AgNPs-LA, and AgNPs-PEG, as demonstrated in Figure 1.

TEM images show the prominence of spherical AgNPs-GSH with a diameter of 2.0 ± 0.4 nm (Figure 2A).

It was also confirmed by SAXRD measurements that peaks location, as received by integration of obtained pattern, show the average distance between metallic cores about 2.2 nm which correspond well with TEM images (in case of SAXRD signal we have to also consider the length of molecules on the surface of nanoparticles so total distance between them is slightly larger). Both methods also

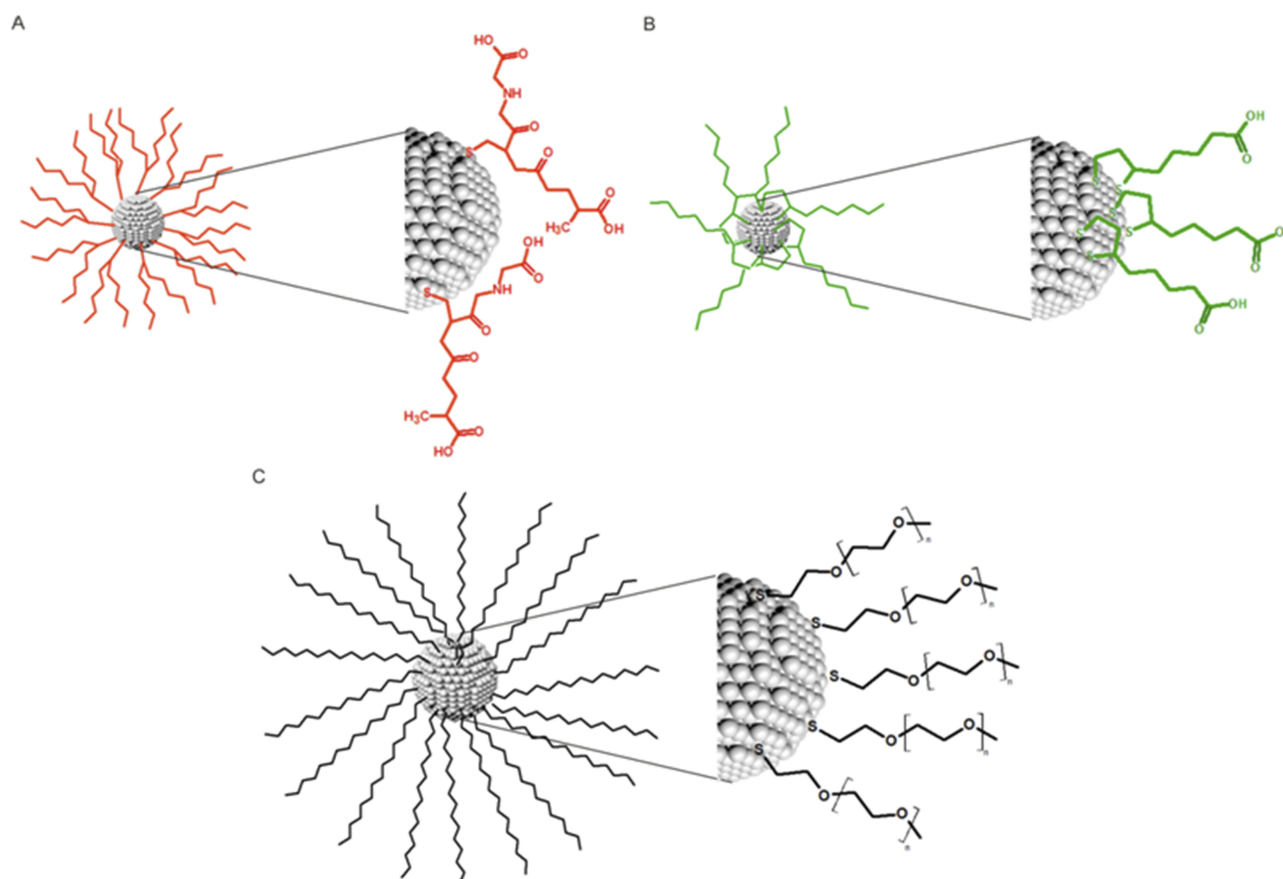


Figure 1 Schematic representation of spherical silver nanoparticles and their surface coverage: (A) 2 nm diameter AgNPs coated with GSH; (B) 2.5 nm diameter AgNPs coated with LA; (C) 3.7 nm diameter AgNPs coated with PEG-2000 Da.

Abbreviations: AgNPs, silver nanoparticles; GSH, glutathione; LA, lipoic acid.

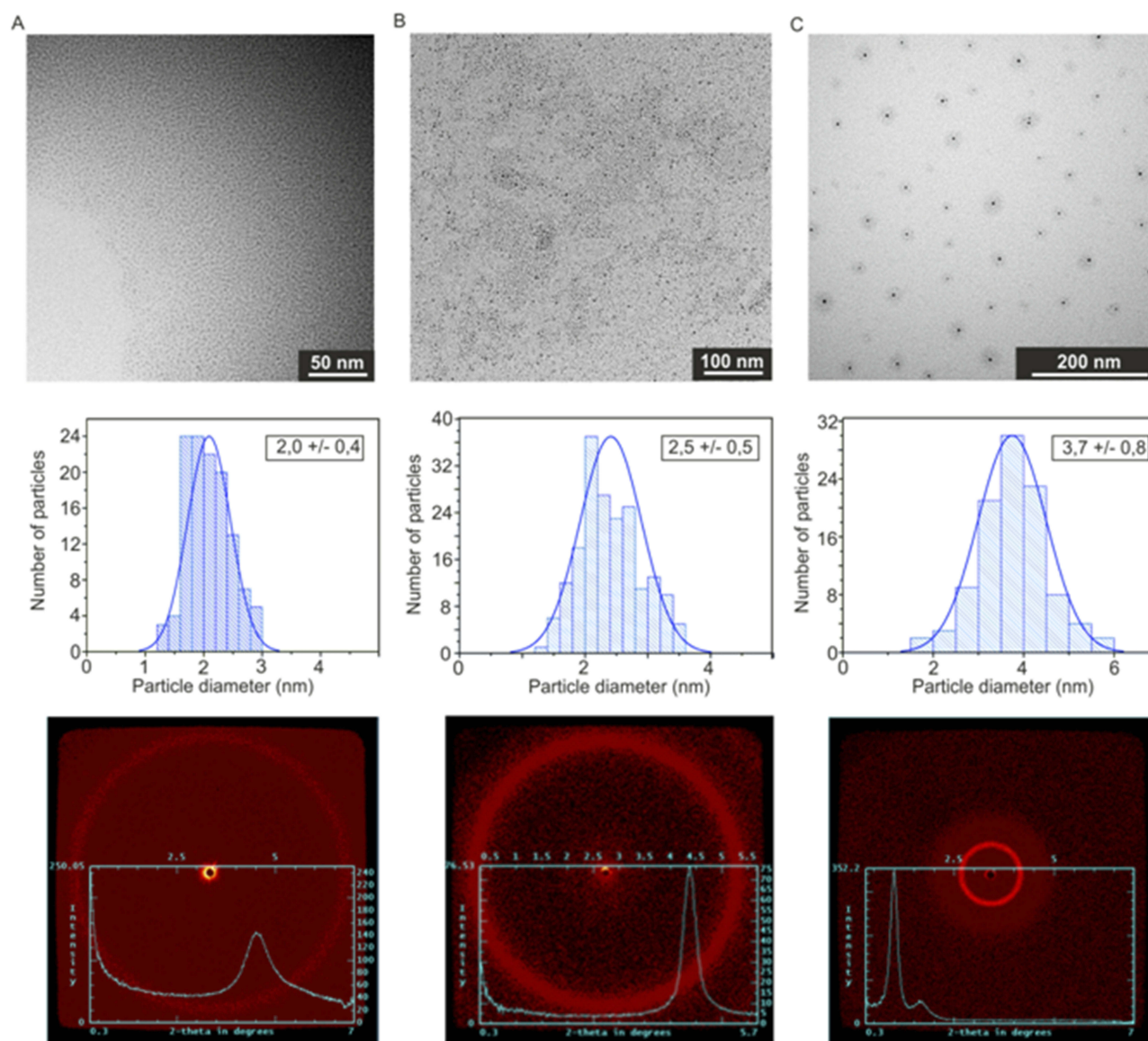


Figure 2 TEM images (top panel), histograms of NPs size distribution (middle panel), and SAXRD patterns (bottom panel): (A) AgNPs-GSH, (B) AgNPs-LA, (C) AgNPs-PEG 2000. **Abbreviations:** TEM, transmission electron microscopy; NPs, nanoparticles; SAXRD, small-angle X-ray diffraction; AgNPs, silver nanoparticles; GSH, glutathione; LA, lipic acid.

consistently confirm the formation of spherical AgNPs-LA and AgNPs-PEG with the average diameter of 2.5 ± 0.5 nm (Figure 2B) and 3.7 ± 0.8 nm (Figure 2C) as calculated by the ImageJ software, respectively. It worth to note that in the attached TEM image, PEG shells around each nanoparticle are clearly visible.

As can be observed in Figure 3, both the spectra of nanoparticles and ligands are characterized by analogous absorption bands, which indicates that the nanoparticles contain the same ligands as compared to controls. Some minor differences may be the result of entanglement of some groups in the molecule in the formation of covalent

bonds on nanoparticles surface or non-covalent in the solid phase under the conditions of FTIR experiments.

To calculate the number of molecules attached to the nanoparticles surface a series of TGA measurements were also performed. Figure 4A–C shows mass loss during when heating the sample. This loss can be attributed to the removal of the organic shell and recalculated to the number of surface thiols. To recalculate the obtained data we first calculated the mass of a single nanoparticle, using the average diameter derived from TEM and the bulk density of the metal. The mass of the organic compounds removed from a single nanoparticle was calculated using

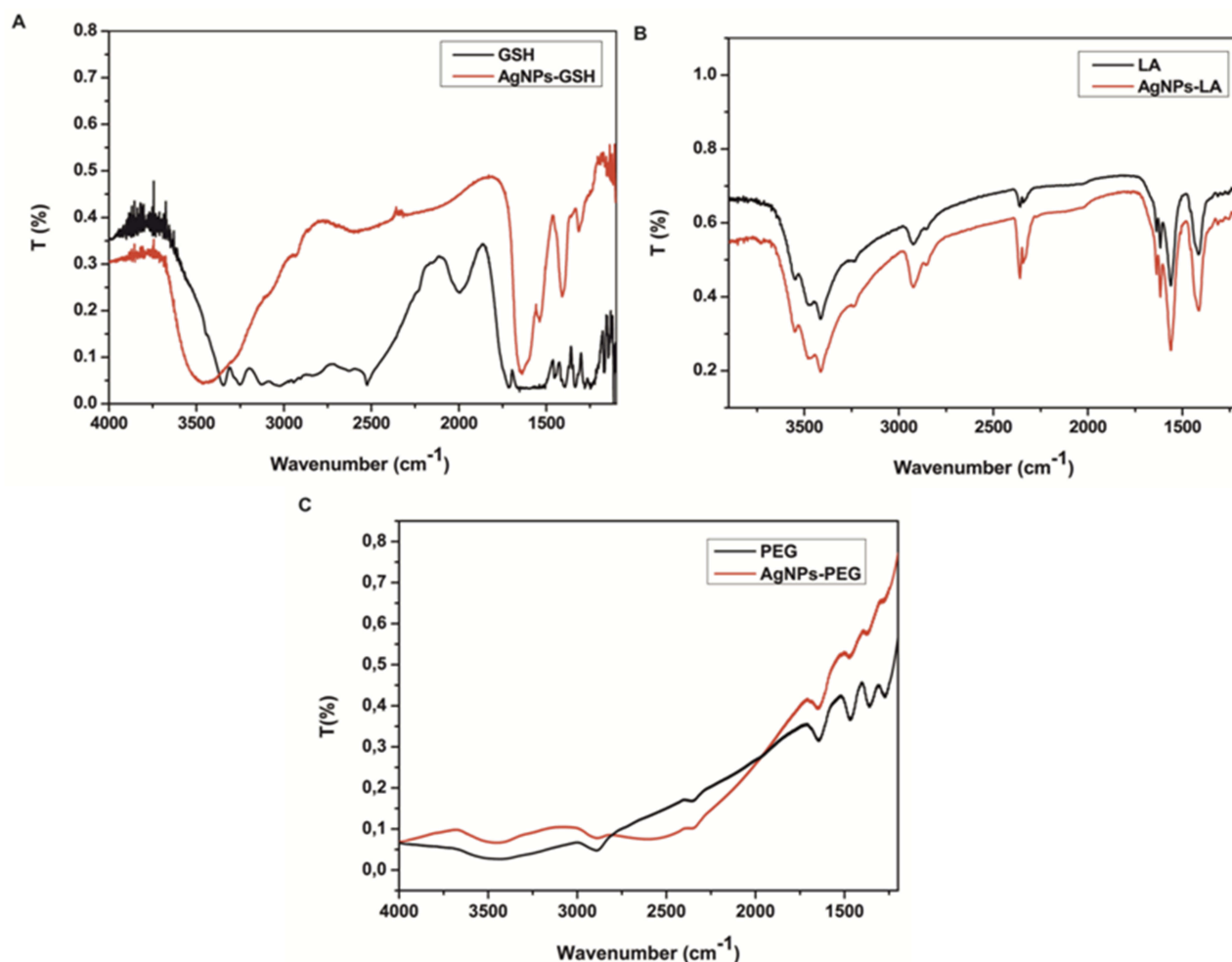


Figure 3 FTIR analysis of (A) AgNPs-GSH, (B) AgNPs-LA and (C) AgNPs-PEG.

Abbreviations: FTIR, Fourier Transform Infrared Spectroscopy; AgNPs, silver nanoparticles; GSH, glutathione; LA, lipoic acid; PEG, polyethylene glycol.

the % of mass left after the analysis. The calculated results are shown in [Table 1](#)

Functionalized AgNPs inhibit platelet aggregation as detected by QCM-D and microscopy

Before each QCM-D experiment platelet viability was confirmed using light aggregometry ([Figure 5A](#)). The perfusion of physiological concentrations of platelets (2.5×10^8 platelets/mL) on polystyrene-coated quartz crystals caused a decrease in frequency and an increase in dissipation indicating the deposition of platelet aggregates on the sensor surface ([Figures 5B](#) and [6](#)). We found that incubation of platelets with AgNPs-GSH and AgNPs-PEG at concentrations 50 and 100 $\mu\text{g/mL}$ or AgNPs-LA at 100 $\mu\text{g/mL}$ significantly decreased dissipation and increased frequency as compared

to controls ([Figures 5B](#) and [6A](#)). The QCM-D data were confirmed by phase contrast microscopy ([Figure 6B](#)).

It is important to note that AgNPs did not cause deposition of plasma proteins on the crystal surface. Indeed, AgNPs did not induce changes in frequency and dissipation when plasma was perfused in the absence of platelets ([Figures 5C](#) and [7](#)).

Moreover, we confirmed that the corresponding concentrations of GSH, LA, and PEG from 10 to 35 μM did not induce changes in dissipation and frequency (data not shown).

Functionalized AgNPs are not cytotoxic for blood platelets for human platelets, endothelial cells, and fibroblasts

The measurement of LDH enzyme release by inhibition of 3-(4, 5-dimethylthiazol-2-yl) 2,5-diphenyl-tetrazolium bromide (MTT) reduction is a commonly used assay to

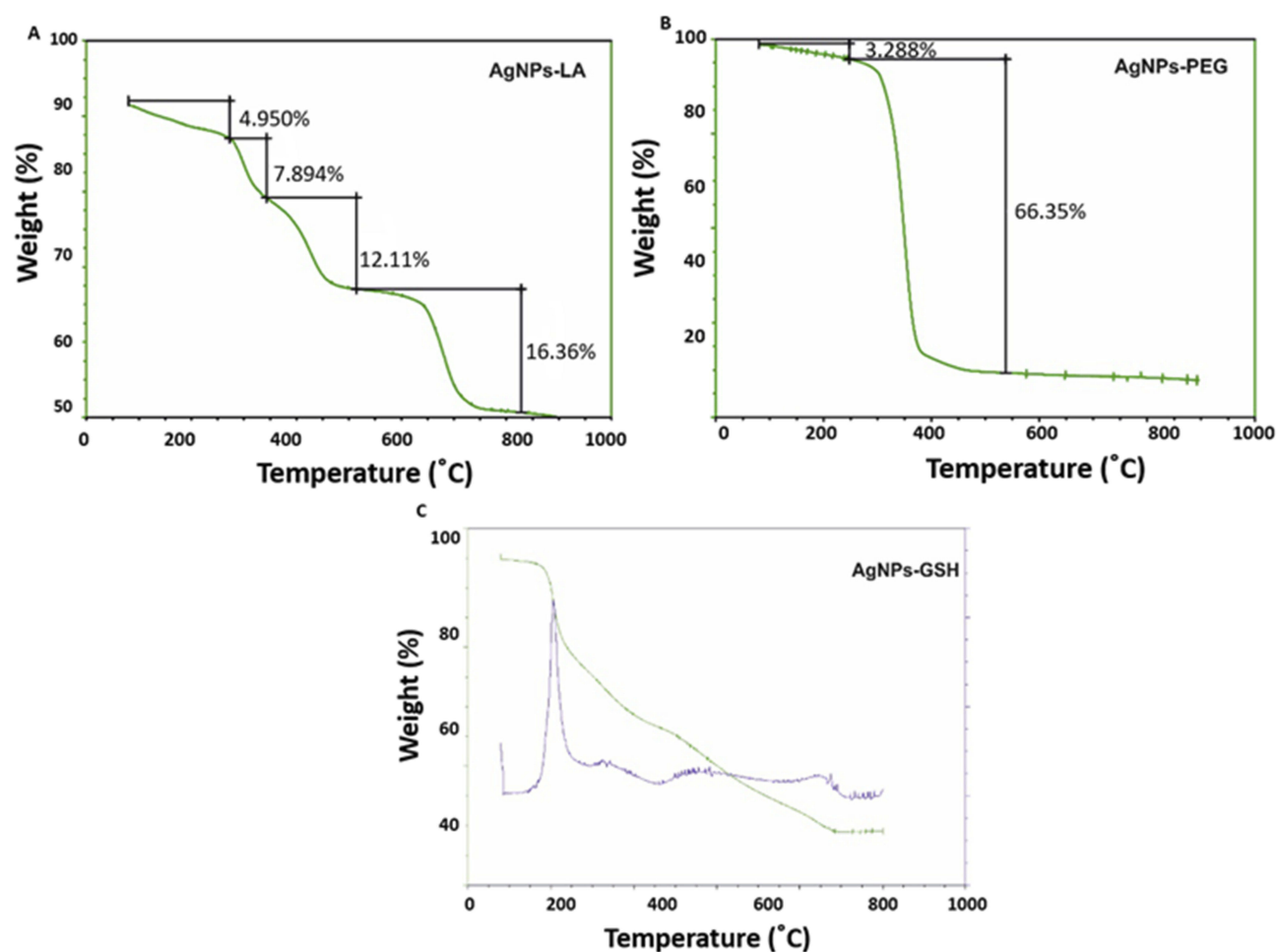


Figure 4 TGA analysis for (A) AgNPs-LA; (B) AgNPs-PEG; (C) AgNPs-GSH.

Abbreviations: TGA, thermogravimetry analysis; AgNPs, silver nanoparticles; LA, lipoic acid; PEG, polyethylene glycol; GSH, glutathione.

Table 1 %mass of organic and number of ligands attached to nanoparticles surface calculated from TGA analysis

Sample	Core size [nm] from TEM	Mas % of organic from TGA	Number of ligands
AgNPs-GSH	2±0.4	48.11	74
AgNPs-LA	2.5±0.5	41.31	176
AgNPs-PEG	3.7±0.8	69.64	192

Abbreviations: TGA, thermogravimetry analysis; TEM, transmission electron microscopy; AgNPs, silver nanoparticles; GSH, glutathione; LA, lipoic acid; PEG, polyethylene glycol.

evaluate potential cytotoxicity following exposure to investigated xenobiotics *in vitro*.²² In our study, the LDH test was chosen because the MTT assay may not be suitable for platelets. Platelets share many of the same biological characteristics as other cells. However, unlike most cells, platelets lack a nucleus and are unable

to adapt to changing biological settings by altered transcription.²³ To exclude possible cytotoxic effect of investigated AgNPs on human platelets, endothelial cells and fibroblasts we measured the release of cytosolic LDH from these cells. LDH is a soluble cytoplasmic enzyme that is present in almost all cells and is released into extracellular space when the plasma membrane is damaged. Necrotic, necroptotic, and late apoptotic cell death are evaluated by determining damage of the plasma membrane.²⁴ Incubation of 2 nm AgNPs-GSH, 2.5 nm AgNPs-PEG, and 3.7 nm AgNPs-LA at concentration of 50 or 100 µg/mL with WPs, for 20 mins and 24 hrs or umbilical vein endothelial cells (HUVEC) and gingival fibroblasts cells (HGF-1) for 24 hrs did not cause a significant release of total LDH (Figure 8). We incubated AgNPs with platelets for 20 mins, i.e., for the duration of our functional assay using QCM-D. The total release of LDH after 24 hrs incubation was higher than after 20

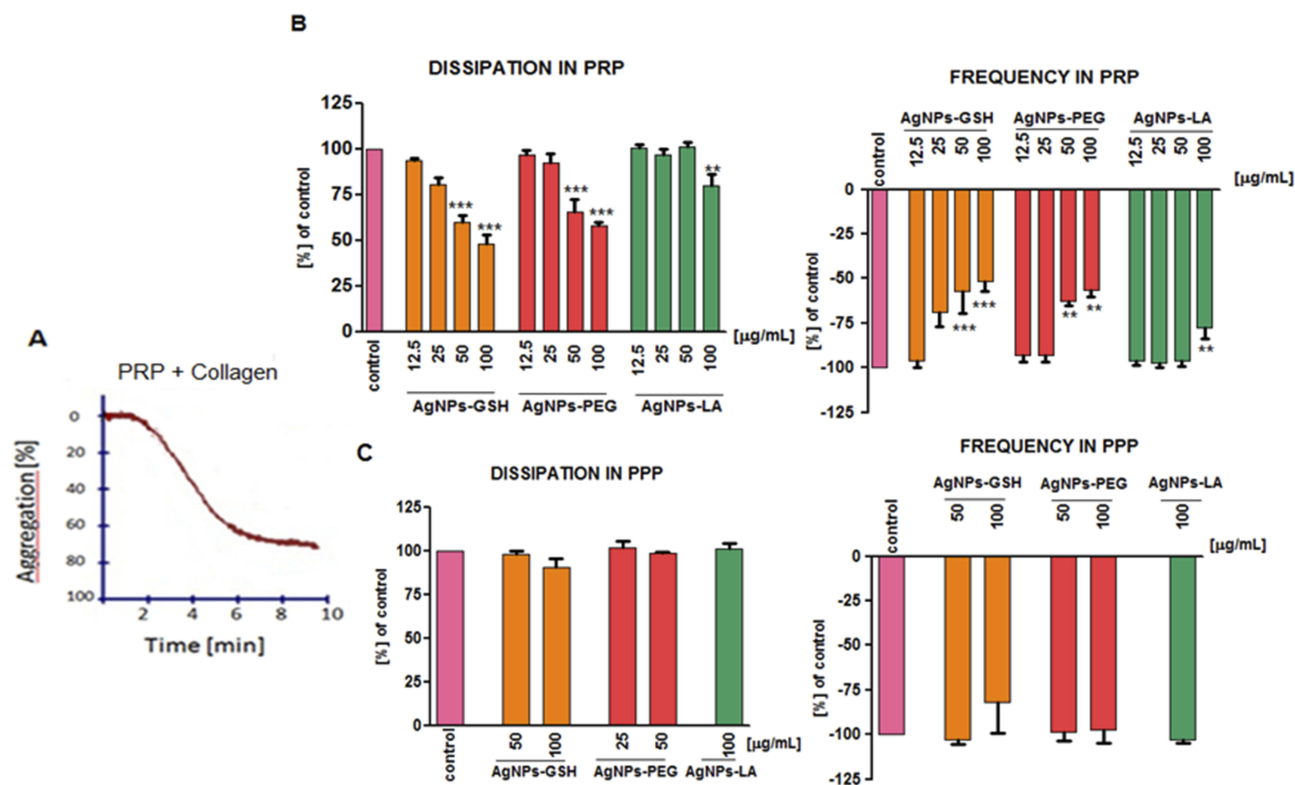


Figure 5 Measurement of the effects of AgNPs on platelet aggregation using light aggregometry and QCM-D.

Notes: (A) A representative light aggregometry tracing showing collagen (2 µg/mL)-induced platelet aggregation. (B) Perfusion of fibrinogen-coated polystyrene-coated quartz crystals with PRP in the presence of AgNPs-GSH, GSH-PEG or AgNPs-LA leads to the reduction of platelet aggregation. (C) Perfusion of fibrinogen-coated polystyrene-coated quartz crystals with PPP in the presence of AgNPs-GSH, GSH-PEG, and AgNPs-LA did not cause significant changes in frequency. Data are expressed as mean \pm standard deviation; $n=4$ ** $P<0.01$; *** $P<0.001$ vs control.

Abbreviations: AgNPs, silver nanoparticles; QCM-D, quartz crystal microbalance with dissipation; PRP, platelet-rich plasma; GSH, glutathione; PEG, polyethylene glycol; LA, lipoic acid; PPP, platelet-poor plasma.

mins, which could be due to the breakdown of platelets. However, the difference between the control and the platelets treated with AgNPs was not significant.

Effects of functionalized AgNPs on the expression of P-selectin and GPIIb/IIIa as measured by flow cytometry

Platelet activation leads to increased abundance of platelet surface receptors such as P-selectin and GPIIb/IIIa.¹⁹ As expected, stimulation of platelets with collagen at 2 µg/mL induced a significant increase in the number of copies of P-selectin and activated GPIIb/IIIa, on the platelet surface. Incubation of PRP with AgNPs-GSH and AgNPs-PEG at 50 and 100 µg/mL or AgNPs-LA at 100 µg/mL significantly inhibited collagen-mediated increase in total P-selectin (Figure 9) and GPIIb/IIIa (Figure 10).

Functionalized AgNPs decrease TXB₂ formation in platelets

Incubation of platelets with AgNPs-GSH and AgNPs-PEG at 50 and 100 µg/mL or AgNPs-LA at 100 µg/mL

significantly inhibited collagen-induced formation of TXB₂ (Figure 11).

Functionalized AgNPs decrease MMP-1 and MMP-2 release from platelets

Collagen at 2 µg/mL caused a significant enhancement of MMP-1 and MMP-2 release in PRP. Incubation of platelets with AgNPs-GSH and AgNPs-PEG significantly inhibited collagen-induced increase in MMP-1 in a concentration-dependent manner and MMP-2 at the highest concentration (100 µg/mL) as indicated in Figure 12.

Based on obtained results, we found that synthesized by our team AgNPs-GSH, AgNPs-PEG, and AgNPs-LA protected against blood platelets aggregation underflow condition and attenuated collagen-mediated increase in total P-selectin and GPIIb/IIIa, TXB₂ formation, MMP-1, MMP-2 release in PRP at concentration non-cytotoxicity to human platelets and human cells at non-cytotoxic concentration (Figure 13).

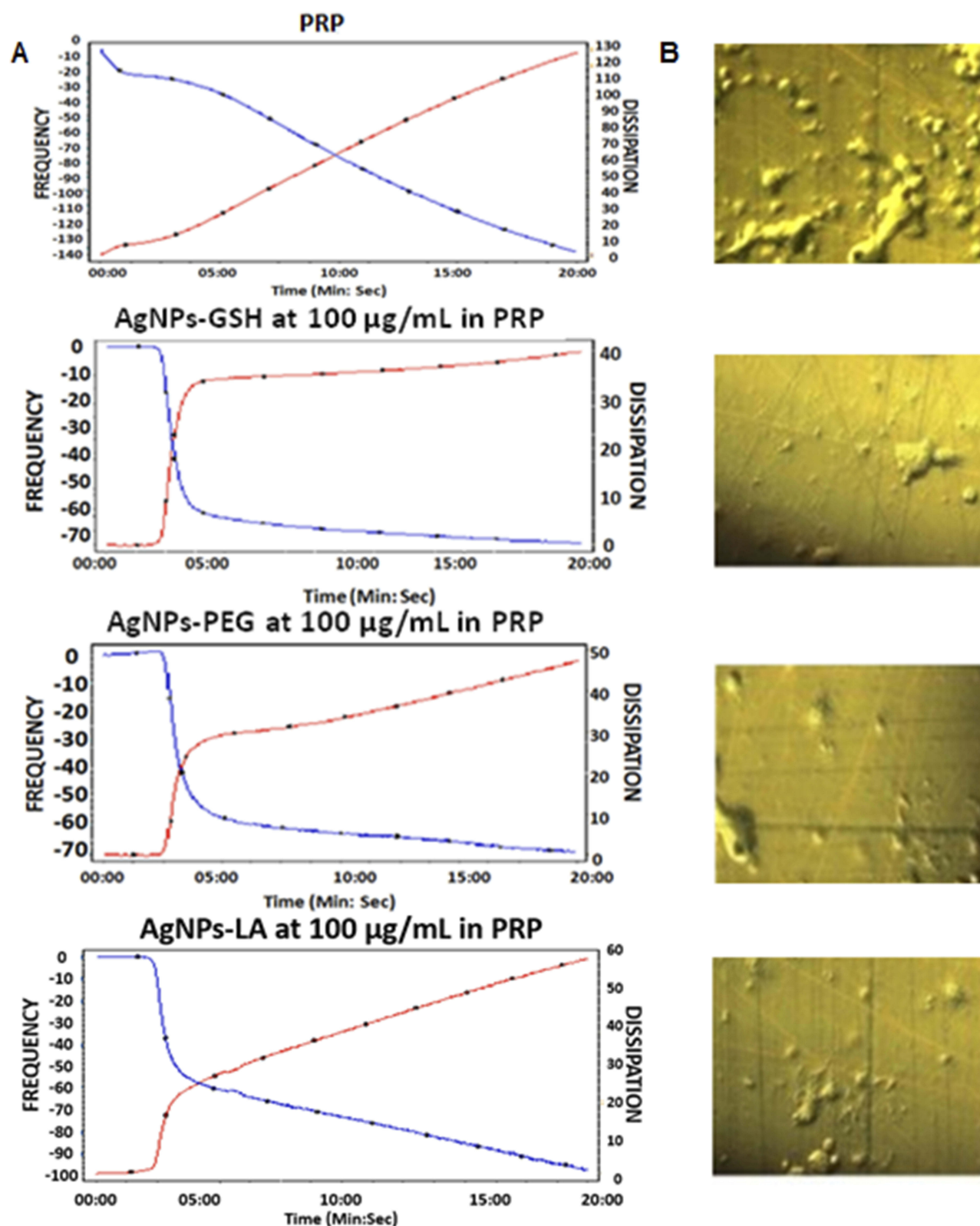


Figure 6 Effects of AgNPs on platelet aggregation as measured by QCM-D. Perfusion of sensor crystals with PRP in the presence of AgNPs-GSH, AgNPs-PEG, or AgNPs-LA (100 $\mu\text{g/mL}$) inhibited platelet aggregation.

Notes: (A) Representative tracings from the third overtone recorded by the device in the presence or absence of AgNPs (100 $\mu\text{g/mL}$) on frequency (blue line, left axis) and dissipation (red line, right axis). (B) Representative micrographs of the surface of sensors as viewed by phase contrast microscopy showing decreased accumulation of platelet aggregates in the presence of AgNPs.

Abbreviations: AgNPs, silver nanoparticles; QCM-D, quartz crystal microbalance with dissipation; PRP, platelet-rich plasma; GSH, glutathione; PEG, polyethylene glycol; LA, lipoic acid.

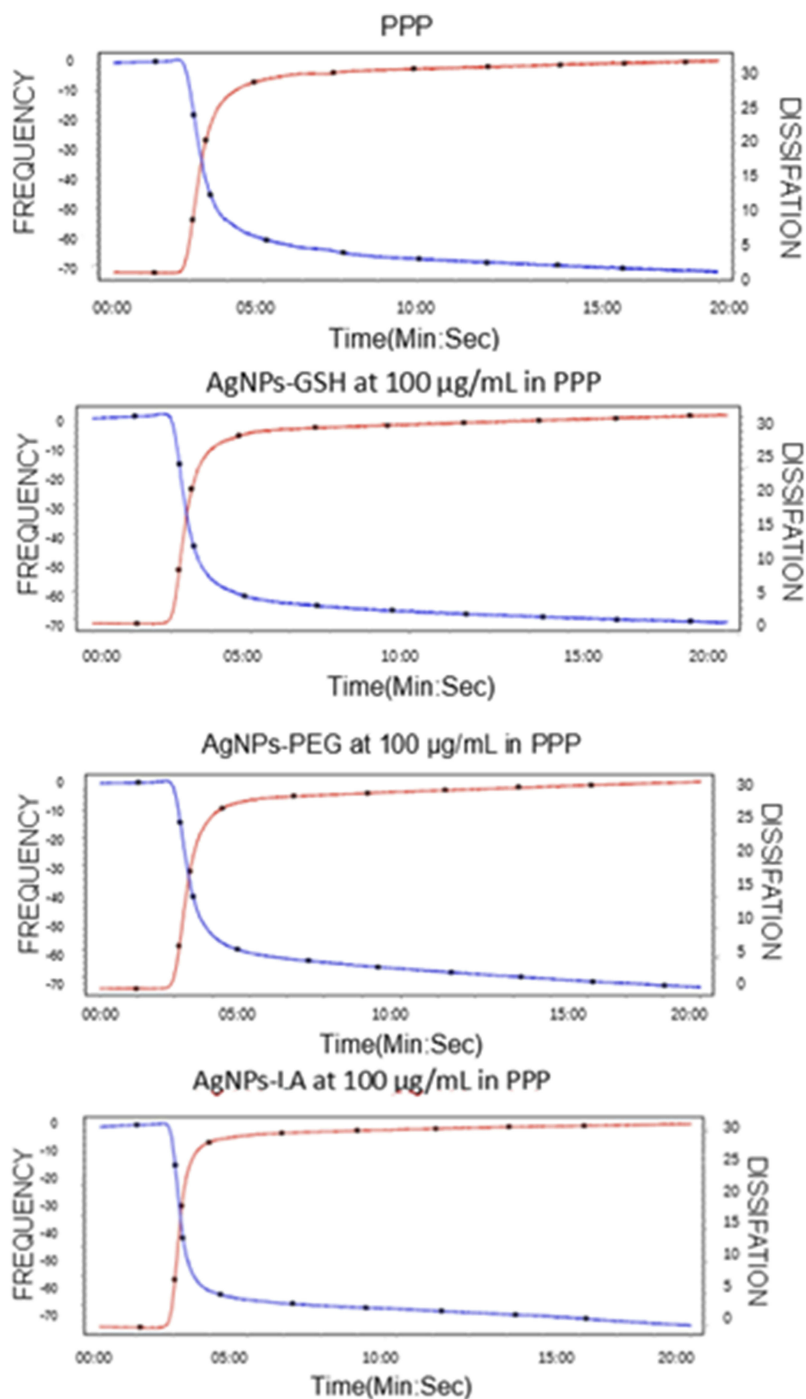


Figure 7 Effects of AgNPs on plasma protein accumulation as measured by QCM-D. In the absence of platelets (PPP) AgNPs did not cause deposition of proteins on the sensor surface. Representative traces from the third overtone recorded by the device showing effects of AgNPs (100 µg/mL) on frequency (blue line, left axis) and dissipation (red line, right axis).

Abbreviations: AgNPs, silver nanoparticles; QCM-D, quartz crystal microbalance with dissipation; PPP, platelet-poor plasma.

Discussion

Both pharmacological and toxicological actions of nanoparticles depend on their functionalization and physico-chemical properties such as shape and size.^{4,12,16,25,26} It has been shown that Ag nanowires (length of 1.5–25 µm;

diameter of 100–160 nm) exerted a strong cytotoxic effect on human lung epithelial A549 cells, whereas spherical AgNPs (30 nm) had negligible effects on the cells.²⁷ The authors suggested that the direct contact of long wires with the cell surface may account for the toxicity. Indeed, we

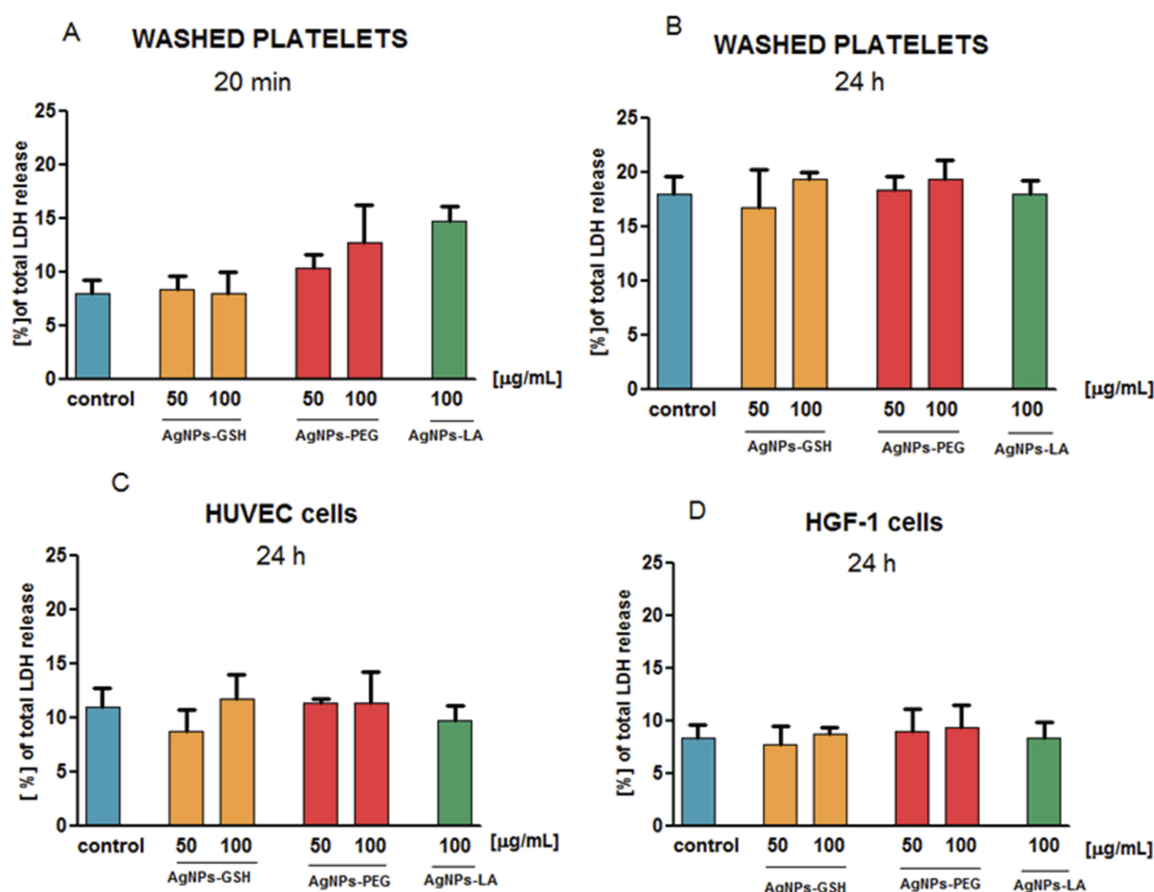


Figure 8 AgNPs do not cause LDH release from (A) washed platelets after 20 mins of incubation, (B) washed platelets, (C) HUVEC, and (D) HGF-1 cells after 24 hrs of incubation as compared with untreated WP or cells. Results are mean \pm standard deviation; $n=3$. Lysis buffer-treated cells and WP were set to 100% (total LDH release). **Abbreviations:** AgNPs, silver nanoparticles; LDH, lactate dehydrogenase; HUVEC, human umbilical vein endothelial cells; WP, washed platelet.

have demonstrated that spherical nanoparticles with the mean size of 2–3.7 nm are not cytotoxic against human cells at concentrations up to 100 $\mu\text{g/mL}$. On the other hand, Helmlinger et al, 2016 demonstrated that toxicity of spheres (20–60 nm), cubes (140–180 nm), and rods (diameter 80–120 nm, length >1000 nm) AgNPs on human mesenchymal cells was not shape dependent.²⁸ Several studies indicated that unmodified nanoparticles of Ag are cytotoxic to human cells.^{26–29} Previously, we have found that treatment of human gingival fibroblast with 2 nm non-functionalized AgNPs causes cells death, apoptosis, inflammation, and oxidative stress.²⁹ We have also documented that exposure to non-functionalized AgNPs with the average size of 18 nm results in nanoparticle uptake by human osteoblast and changes in cell ultrastructure leading to apoptosis and necrosis. Moreover, the cell death was associated with increased level of iNOS mRNA, iNOS protein, and generation of increased amounts of NO.²⁶ In contrast, functionalized Ag nanoparticles may

be more biocompatible.^{4,5,8,10,13–16,30,31} A number of strategies are available to increase the biocompatibility of nanoparticles. Pegylation, i.e., coating the surface of nanoparticles with PEG is a commonly used approach for improving the efficiency of drug delivery to target cells and tissues. PEG coatings on nanoparticles shield the surface from aggregation and prolong systemic circulation time.³² Glutathione is present in human tissues as the most abundant nonprotein thiol that defends against oxidative stress and it plays an important role in the detoxification processes.³³ In some studies, GSH was used as a stabilizer of nanoparticles.^{33–36} Finally, LA, well known as an antioxidant, and agent improving biocompatibility of nanoparticles.³⁷ Also, our previous study demonstrated that 10 nm AgNPs functionalized with LA and PEG were less toxic against human gingival fibroblast in vitro than the unmodified ones.¹⁶ Therefore, we synthesized GSH-PEG- and LA-functionalized AgNPs and studied the effects of these nanoparticles on platelet function. We

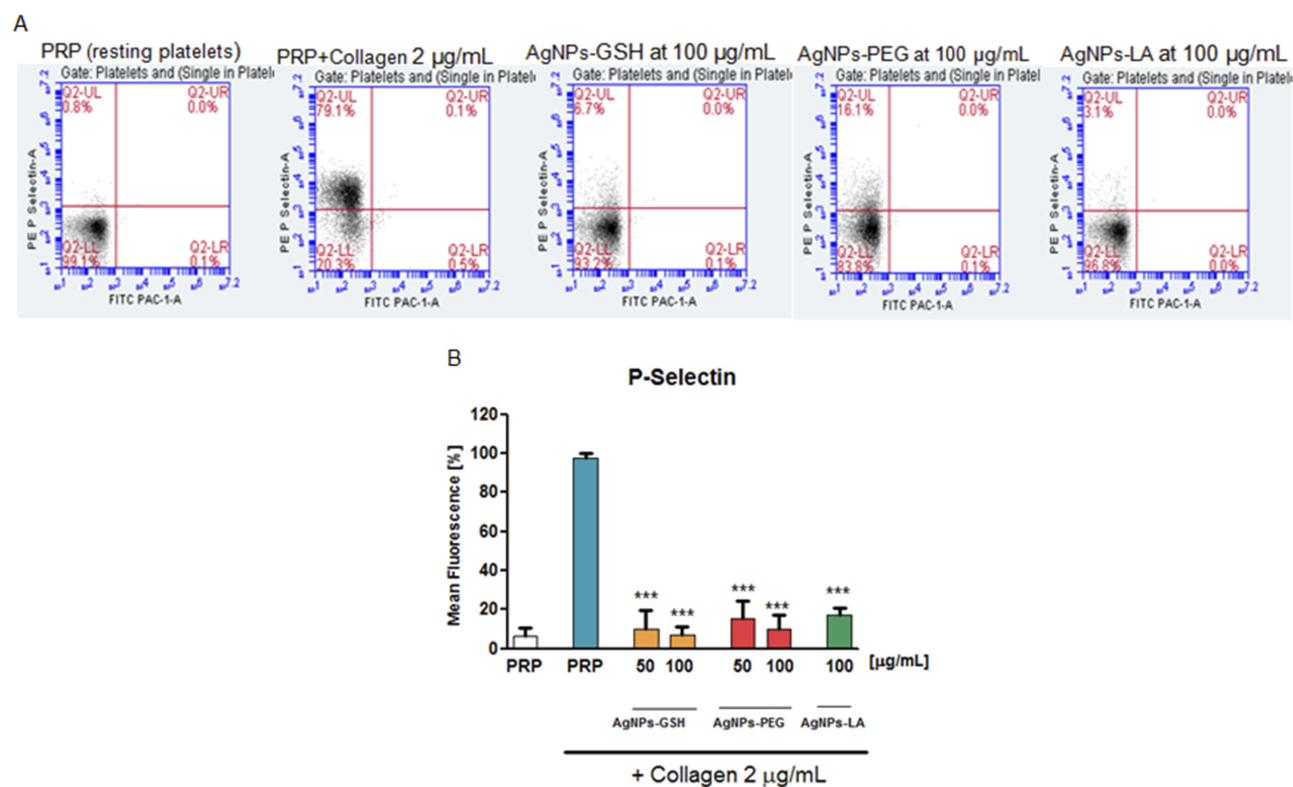


Figure 9 AgNPs-GSH, AgNPs-PEG, and AgNPs-LA attenuated collagen-stimulated increase in the abundance of P-selectin on the platelets.

Notes: (A) Representative flow cytometry recordings showing effects of AgNPs-GSH, AgNPs-PEG, and AgNPs-LA (100 $\mu\text{g/mL}$) on P-Selectin. The corresponding bar graph shows an analysis of the effects of AgNPs on (B) P-Selectin. Data are expressed as mean \pm standard deviation; n=4; *** p <0.001 vs collagen-stimulated platelets or as indicated.

Abbreviations: AgNPs, silver nanoparticles; GSH, glutathione; PEG, polyethylene glycol; LA, lipoic acid.

found that all tested functionalized AgNPs exerted antiplatelet properties at non-cytotoxic concentrations as measured by QCM-D. The QCM-D method is able to measure nanoparticle-induced platelet microaggregation, underflow, mimicking conditions encountered in microvasculature, at concentrations undetectable by light aggregometry and flow cytometry.^{20,21} Consistent with our results, Ragaseema et al, 2012 observed inhibitory effect of PEG-coated AgNPs on platelets aggregation.⁸ In other research, 10 nm AgNPs showed dose-dependent antiplatelet activity and decreased ADP-induced aggregation as measured by light aggregometry.³⁰ Moreover, Shrivastava et al, 2009 presented that 10–15 nm AgNPs showed antiplatelet both in vitro and in vivo.³⁸ In contrast, 10–100 nm AgNPs-induced platelet aggregation both in isolated human platelets and in an animal model following intratracheal instillation.⁶ Huang et al 2016 demonstrated that 20 nm AgNPs coated with polyvinyl pyrrolidone and citrate at the concentration of 500 $\mu\text{g/mL}$ exerted no significant effect on human platelet aggregation.⁵ Similarly, in 18 healthy human volunteers, after 2 weeks of daily exposure to orally ingested commercial 32 nm AgNPs, no effect on

platelet aggregation was detected by light transmission aggregometry at peak serum silver concentrations <10 $\mu\text{g/L}$.⁹ These contradictory results, i.e., inhibition, stimulation, or no significant effect of AgNPs on platelet function may be due to differences in the size of AgNPs, their stabilization, functionalization, as well as method of synthesis.

Mechanisms underlying modulation of platelet function by AgNPs might result from their cytotoxic effects. Some researchers found that AgNPs, can induce inflammation, oxidative stress, ultrastructural alteration, or apoptosis.^{15,38} However, our findings do not support the notion that platelet-inhibitory effects of functionalized AgNPs are due to their cytotoxic effects as all three cell types: platelets, endothelial cells, and fibroblasts when exposed to these nanoparticles did not show cytotoxicity as measured by LDH release. This is consistent with work of Shrivastava et al, 2009 who confirmed that 10–15 nm AgNPs even at higher concentration (500 $\mu\text{g/mL}$), did not affect platelet membrane integrity.³⁹ Similarly, Krishnaraj and Berchmans, 2013 did not observe LDH release from platelets after exposure to 10 nm AgNPs at the

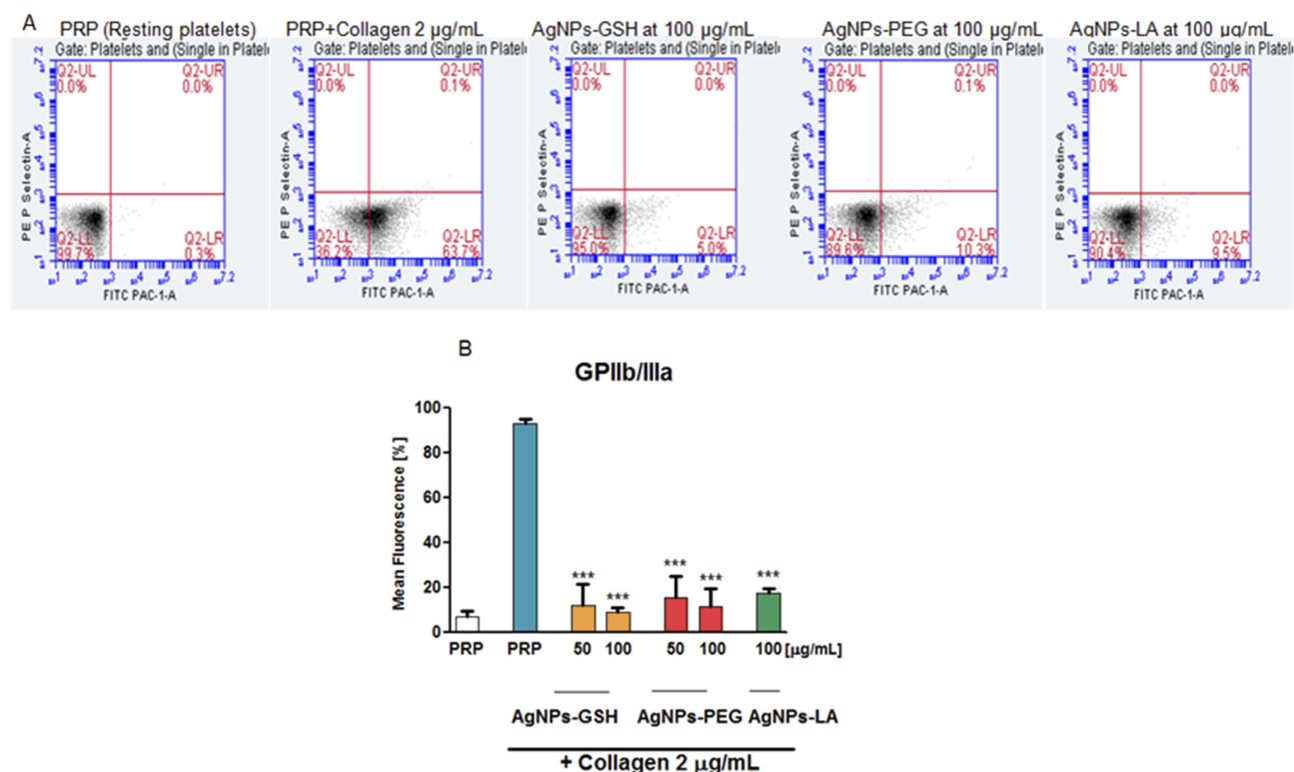


Figure 10 AgNPs-GSH, AgNPs-PEG, and AgNPs-LA attenuated collagen-stimulated increase in the abundance of GPIIb/IIIa on the platelet surface.

Notes: (A) Representative flow cytometry recordings showing effects of AgNPs-GSH, AgNPs-PEG, and AgNPs-LA (100 $\mu\text{g/mL}$) on GPIIb/IIIa. The corresponding bar graph shows analysis of the effects of AgNPs on (B) GPIIb/IIIa. Data expressed as mean \pm standard deviation; $n=4$; *** $P<0.001$ vs collagen-stimulated platelets or as indicated.

Abbreviations: AgNPs, silver nanoparticles; GSH, glutathione; PEG, polyethylene glycol; LA, lipoic acid.

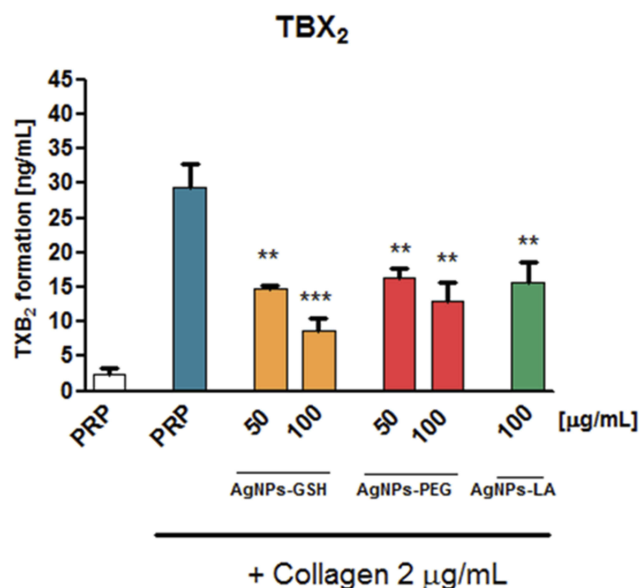


Figure 11 AgNPs-GSH, AgNPs-PEG, and AgNPs-LA decreased collagen-induced formation of TXB₂ by platelets.

Notes: Data expressed as mean \pm standard deviation; $n=4$; ** $P<0.01$; *** $P<0.001$ vs collagen-stimulated platelets.

Abbreviations: AgNPs, silver nanoparticles; GSH, glutathione; PEG, polyethylene glycol; LA, lipoic acid.

concentration range of 0.9–3.5 nM.⁴⁰ Furthermore, Kim et al, 2008 reported that nanosilver up to 300 mg/kg was nontoxic to rodents.³⁸

It is rather more likely that platelet-inhibitory effects of functionalized AgNPs are due to interactions with platelet surface proteins. Platelet activation alters the composition of the platelet membrane, leading to surface expression of P-selectin and an increase in the number of integrin GPIIb/IIIa.^{19,41} The activation of GPIIb/IIIa receptor is a common pathway leading to platelet activation and is also targeted by nanoparticles.⁴² Indeed, in the current experiments, all tested functionalized AgNPs inhibited activation of GPIIb/IIIa on the platelet surface. Furthermore, it has been shown that the inhibition of platelets aggregation by AgNPs could be due to conformational modulation of platelet surface integrins GPIIb/IIIa.⁴¹ Therefore, we propose that platelet-inhibitory activity of functionalized AgNPs is due to interactions with the function of this receptor complex. In addition to inhibition of activation of GPIIb/IIIa functionalized AgNPs may inhibit agglutination, i.e., passive mechanism of platelet

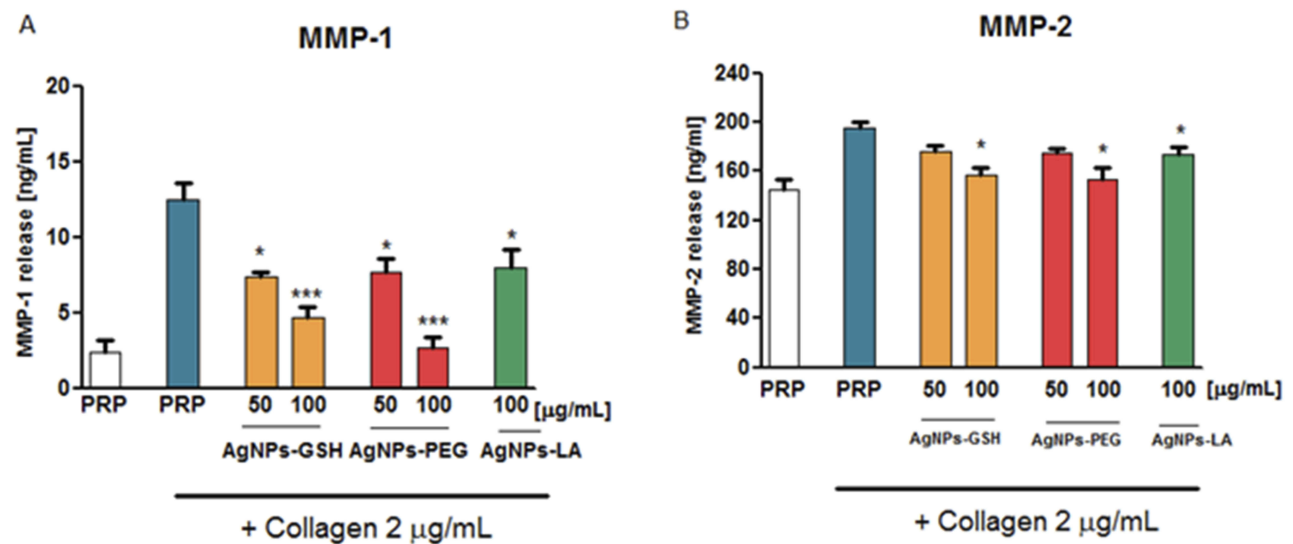


Figure 12 AgNPs-GSH, AgNPs-PEG, and AgNPs-LA attenuated collagen-induced increase of (A) MMP-1 and (B) MMP-2 levels from platelets.

Notes: Data expressed as mean \pm standard deviation; n=4; * P <0.05; *** P <0.001 vs collagen-stimulated platelets or as indicated.

Abbreviations: AgNPs, silver nanoparticles; GSH, glutathione; PEG, polyethylene glycol; LA, lipoic acid.

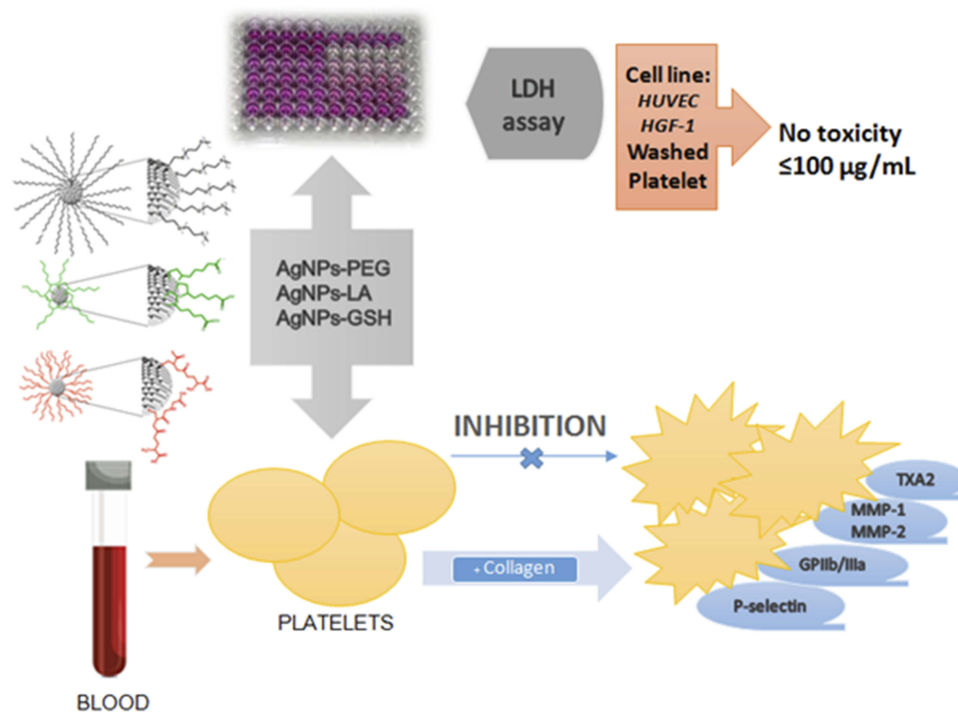


Figure 13 Effects of functionalized AgNPs on human platelet aggregation.

Abbreviation: AgNPs, silver nanoparticles.

aggregation.⁴³ Nanoparticle-induced platelet agglutination depends on the formation of nanoparticle–nanoparticle aggregates and these facilitate nanoparticle-made bridge formation between.⁴⁴ As functionalized AgNPs form less nanoparticle aggregates than uncoated NPs this property

could also contribute to mechanisms that underlie the platelet-inhibitory activity of these NPs.

Finally, the net charge of functionalized AgNPs in interactions with platelets should be considered. Indeed, Dobovolskaia and colleagues showed that cationic but not

neutral or anionic PAMAM dendrimers have the ability to stimulate platelet aggregation. In our experiments, we used three types of organic molecules as surface ligands to modify nanoparticles: PEG-SH, α -LA, and L-Glutathione. Because thiol group of PEG-SH molecule creates a bond between the surface of the nanoparticle and the PEG moiety, it is not involved in any acid–base relationship. PEG stabilized nanoparticle should be considered as a neutral particle, which net charge cannot be influenced by acid or based environment. Moreover, PEG-ylated nanoparticles in contrast to other types of nanoparticles are subjected to well-known biological effects related to much weaker binding of macromolecules from physiological media. A weak interference of PEGylated nanoparticles with the immune system has been linked to the lower degree of protein binding to particles and prevents unwanted biological effects in many drug delivery systems based on this type of nanoparticles.⁴⁵ Coating of NPs with bulky molecules like PEG decreases protein binding to NPs as well as phagocytosis.⁴⁶ Therefore, the presence of PEG on the surface of PEG-AgNPs could limit interactions between platelet receptors such as GPIIb/IIIa and their ligands thus inhibiting platelet aggregation. The functionalization of AgNPs with GSH or LA may result in negative surface charge of GSH-AgNPs and LA-AgNPs. For α -LA, there is only one part of the molecule that can be protonated and deprotonated – it is carboxylic group which $pK_a = 4.52$, therefore in the biological experiment this molecule is deprotonated and gives negative net charge to the whole nanoparticle. The situation is more complicated for glutathione-stabilized nanoparticles because for L-GSH reduced pK_a can be distinguished: $pK_1 = 2.12$ (COOH), $pK_2 = 3.59$ (COOH), $pK_3 = 8.75$ (NH₂), $pK_4 = 9.65$ (SH). According to these data, GSH has a net negative charge at neutral pH and is highly water soluble. Therefore, it would be expected to reside in an aqueous environment and has less absorption on cell membranes. The influence of surface charge is difficult to interpret for GSH because effective surface charge may be modulated in physiological solution due to binding of proteins that have significant affinity to glutathione, very common molecule for cell environment. As an increase in platelet negative surface charge decreases platelet aggregation, platelet surface charge effects of GSH-AgNPs and LA-AgNPs could contribute to inhibition of platelet aggregation by these nanoparticles.⁴⁷ The function of platelet receptors is regulated by a number of downstream platelet mediators.

In the previous studies, it was indicated that the platelet release of MMP-1 and MMP-2 was caused by collagen-induced aggregation.^{48,49} These MMPs rapidly relocate from granule structures inside the platelet to the plasma membrane of activated platelets and enhance P-selectin expression, platelet procoagulant activity, and thrombus formation.^{48–51} Moreover, MMP-2 is involved in the modification of platelet glycoprotein $\alpha_{IIb}\beta_3$ resulting in enhanced platelet adhesion and aggregation.^{48,49,52} MMP-1 was also indicated to associate with the $\alpha_{IIb}\beta_3$ integrin, as suggested by Galt et al, 2002.⁵² It has been shown that MMP-2 contributed to platelets stimulation and aggregation by non-ADP and non-TXA₂ pathway.^{51,53}

Thromboxane A₂ is yet another platelet mediator that acts as a potent vasoconstrictor and a stimulator of platelet aggregation. We found that all tested functionalized AgNPs, similar to aspirin, which represents commonly used antiplatelet agent, may exert a part of their effects through reduction of TXA₂ production.⁵¹ Interestingly, Falcinelli et al, 2007 indicated that the lack of aspirin intake on MMP-2 release in vivo is probably implicated in the mechanism of aspirin resistance.⁵³ Thus, synthesized by our team functionalized AgNPs as inhibitors of MMP-2 and MMP-1 would be suggested as a novel, alternative strategy for developing therapeutics in thrombosis.^{54–57} Furthermore, due to critical role in inducing platelet aggregate formation, GPIIb/IIIa has become a primary target for the development of antithrombotic agents. Currently, three integrin GPIIb/IIIa antagonists (abciximab, eptifibatide, and tirofiban) have been approved for clinical use.⁵⁸ Unfortunately, they exert severe side effects, especially bleeding complications and therefore studies on the development of more effective and safer antiplatelet agents are needed.

One needs to acknowledge that a significant limitation when developing functionalized AgNPs as antiplatelet agents may be due to the fact that non-functionalized may exert opposite effects and activate platelets. Indeed, Jun et al, 2011 observed that 10–100 nm AgNPs at a concentration of 100–250 $\mu\text{g/mL}$ induced platelet activation and increase of P-selectin expression under in vitro condition. Moreover, they found that exposure of rats to AgNPs (0.05–0.1 mg/kg i.v. or 5–10 mg/kg intratracheal instillation) enhanced P-selectin expression.⁶ Therefore, careful pharmacokinetics studies examining the fate of functionalized AgNPs would be crucial for pharmacological development of these agents.

According to the International Organization for Standardization (ISO 10993-4), five different categories (thrombosis, coagulation, platelets, hematology, and immunology (complement system and leukocytes)), are necessary for hemocompatibility evaluation.⁵⁹

Our studies estimate influence for them, i.e., platelets and endothelial cells, which may suggest hemocompatibility. There is no doubt that to precisely define the safety profile of those AgNPs further studies for evaluating their effect on erythrocytes and white cells are warranted. Other authors have studied the effect of AgNPs to morphological blood elements that are also part of the immune system (NK cells, lymphocyte). These immune cells are belonging to the innate immune system and they can be rapidly activated upon recognition of a foreign invader such as a foreign material. So far, AgNPs affected the enzymatic and non-enzymatic antioxidant systems of red blood cells (RBCs), additionally were toxic at a high concentration, against low concentration (<0.4 µg/mL) of AgNPs was relatively safe.⁶⁰ Also exposure to AgNPs of NK cells, reduced the viability and the cytotoxic potential after poly-riboinosinic-polyribocytidylic acid stimulation of NK cells and increased the expression of the inhibitory receptor CD159a. In the same, studies were confirmed that exposure to AgNPs changes NK cells' function and phenotype and may present a risk for modulating human immune responses.⁶¹ For comparison, l-cysteine functionalized silver do not exhibit acute toxicity for plasma after intragastric and intraperitoneal administration.⁶² Similarly, in Ferrer's research AgNPs functionalized with dextran did not affect morphology and cell viability of monocytes (THP-1).⁶³ But, another study shows that for RBCs, AgNP-PVP-20 at ~40 µg/mL could cause hemolysis to 19%. Both AgNP-PVP-20 and AgNP-CIT-20 were quite toxic to lymphocytes since they severely inhibited both lymphocyte proliferation and viability.⁶⁴

Limitations and future perspectives

As it is an in vitro investigation, studies exploring, pharmaceutical, pharmacological, therapeutic, and clinical potential of functionalized AgNPs need to be performed. However, it is clear that the modification of AgNPs by functionalization holds a promise for further development of AgNPs as pharmaceutical or imaging agents. Having regard to successful clinical applications, it is necessary to precisely define safety profiles of AgNPs, therefore, effect of their exposure is a key issue that needs further in vivo assessment.⁶⁵

Conclusion

We have shown that functionalized AgNPs (AgNPs-GSH, AgNPs-PEG, and AgNPs-LA) sized from 2 to 3.7 nm inhibit platelet aggregation underflow condition. Mechanisms of this action of functionalized AgNPs are likely to be dependent on down-regulation of P-selectin and GPIIb/IIIa receptor expression, TXA₂ formation, and MMP-1, MMP-2 release from platelets. Figure 13 summarizes the effects of functionalized AgNPs on platelets.

We believe that these findings are important for understanding interactions between AgNPs and human platelets and their pharmacological and toxicological significance. The lack of cytotoxicity against the important elements of the circulation system, i.e., platelets and endothelial cells in LDH assay, suggests potential hemocompatibility. Further studies are warranted for establishing the safety profile of these AgNPs prior to their potential clinical applications.

Acknowledgments

This work was funded by the National Science Centre of Poland HARMONIA grant: 2017/26/M/NZ7/01030. Nadhim Kamil Hante is funded from the Ministry of Higher Education and Scientific Research in Iraq (MoHER).

Disclosure

The authors report no conflicts of interest in this work.

References

1. Lee SH, Jun BH. Silver nanoparticles: synthesis and application for nanomedicine. *Int J Mol Sci*. 2019;20:4.
2. Rai M, Kon K, Ingle A, Duran N, Galdiero S, Galdiero M. Broad-spectrum bioactivities of silver nanoparticles: the emerging trends and future prospects. *Appl Microbiol Biotechnol*. 2014;98(5):1951–1961. doi:10.1007/s00253-013-5473-x
3. Pudlacz A, Szemraj J. Nanoparticles as carriers of proteins, peptides and other therapeutic molecules. *Open Life Sci*. 2018;13:285–298. doi:10.1515/biol-2018-0035
4. Santos-Martinez MJ, Rahme K, Corbalan JJ, et al. Pegylation increases platelet biocompatibility of gold nanoparticles. *J Biomed Nanotechnol*. 2014;10(6):1004–1015.
5. Huang H, Wenjia L, Menghua C. An evaluation of blood compatibility of silver nanoparticles. *Sci Rep*. 2016;6(255180):1–15.
6. Jun EA, Lim KM, Kim KY. Silver nanoparticles enhance thrombus formation through increased platelet aggregation and procoagulant activity. *Nanotoxicology*. 2011;5(2):157–167. doi:10.3109/17435390.2010.506250
7. Shrivastava S, Singh S, Mukhopadhyay A. Negative regulation of fibrin polymerization and clot formation by nanoparticles of silver. *Colloids Surf B*. 2011;82(1):241–246. doi:10.1016/j.colsurfb.2010.08.048
8. Ragaseema VM, Unnikrishnan S, Kalliyana Krishnan V, Krishnan LK. The antithrombotic and antimicrobial properties of PEG-protected silver nanoparticle coated surfaces. *Biomaterials*. 2012;33(11):3083–3092. doi:10.1016/j.biomaterials.2012.01.005

9. Smock KJ, Schmidt RL, Hadlock G, Stoddard G, Grainger DW, Munger MA. Assessment of orally dosed commercial silver nanoparticles on human ex vivo platelet aggregation. *Nanotoxicology*. 2014;8(3):328–333.
10. Thasneem YM, Sajeesh S, Sharma C. Effect of thiol functionalization on the hemo-compatibility of PLGA nanoparticles. *J Biomed Mater Res*. 2011;99A(4):607–617. doi:10.1002/jbm.a.33220
11. Jokerst JV, Lobovkina T, Zare RN, Gambhir SS. Nanoparticle PEGylation for imaging and therapy. *Nanomedicine*. 2011;6(4):71. doi:10.2217/nnm.11.19
12. Petros RA, DeSimone JM. Strategies in the design of nanoparticles for therapeutic applications. *Nat Rev Drug Discov*. 2010;9(8):615–627. doi:10.1038/nrd2591
13. Milla P, Dosio F, Cattel L. PEGylation of proteins and liposomes: a powerful and flexible strategy to improve the drug delivery. *Curr Drug Metab*. 2012;13(1):105–119. doi:10.2174/138920012798356934
14. Niidome T, Yamagata M, Okamoto Y, et al. PEG-modified gold nanorods with a stealth character for in vivo applications. *J Control Release*. 2006;114(3):343–347. doi:10.1016/j.jconrel.2006.06.001
15. Nguyen KC, Seligy VL, Massarsky A, et al. Comparison of toxicity of uncoated and coated silver nanoparticles. *J Phys*. 2013;429:1–15.
16. Niska K, Knap N, Kędzia A, Jaskiewicz M, Kamysz W, Inkielewicz-Stepniak I. Capping agent-dependent toxicity and antimicrobial activity of silver nanoparticles: an in vitro study. Concerns about potential application in dental practice. *J Med Sci*. 2016;13(10):772–782.
17. Chen Y, Wang X. Novel phase-transfer preparation of monodisperse silver and gold nanoparticles at room temperature. *Mater Lett*. 2008;62(15):2215–2218. doi:10.1016/j.matlet.2007.11.050
18. Van der Linden M, Barendregt A, van Bunningen AJ. Characterisation, degradation and regeneration of luminescent Ag₂₉ clusters in solution. *Nanoscale*. 2016;8(47):19901–19909. doi:10.1039/C6NR04958C
19. Radomski MW, Moncada S. An improved method for washing of human platelets with prostacyclin. *Thromb Res*. 1983;30:383–389. doi:10.1016/0049-3848(83)90230-X
20. Santos-Martinez MJ, Inkielewicz-Stepniak I, Medina C, et al. The use of quartz crystal microbalance with dissipation (QCM-D) for studying nanoparticle-induced platelet aggregation. *Int J Nanomedicine*. 2012;7:243–255. doi:10.2147/IJN.S30631
21. Santos-Martinez MJ, Tomaszewski KA, Medina C, Bazou D, Gilmer JF, Radomski MW. Pharmacological characterization of nanoparticle-induced platelet microaggregation using quartz crystal microbalance with dissipation: comparison with light aggregometry. *Int J Nanomedicine*. 2015;10:5107–5119.
22. Niles AL, Moravec RA, Riss TL. In vitro and cytotoxicity testing and same-well multi-parametric combinations for high throughput screening. *Curr Chem Genomics*. 2009;3:33–41. doi:10.2174/1875397300903010033
23. Xu X, Gao X, Pan R, Lu D, Dai Y. A simple adhesion assay for studying interactions between platelets and endothelial cells in vitro. *Cytotechnology*. 2010;61(1):17–22. doi:10.1007/s10616-010-9256-2
24. Ka-Ming Chan F, Moriwaki K, De Rosa MJ. Detection of necrosis by release of lactate dehydrogenase 9LDH activity. *Methods Mol Biol*. 2013;979:65–70.
25. Laloy J, Minet V, Alpan L. Impact of Silver nanoparticles on haemolysis, platelet function and coagulation. *Nanobiomedicine*. 2014;1:4. doi:10.5772/59346
26. Zielinska E, Tukaj C, Radomski MW, Inkielewicz-Stepniak I. Molecular mechanism of silver nanoparticles-induced human osteoblast cell death: protective effect of inducible nitric oxide synthase inhibitor. *PLoS One*. 2016;11(10):e0164137. doi:10.1371/journal.pone.0164137
27. Stoehr LC, Gonzalez E, Stampfl A, et al. Shape matters: effects of silver nanospheres and wires on human alveolar epithelial cells. *Part Fibre Toxicol*. 2011;8:36. doi:10.1186/1743-8977-8-36
28. Helmlinger J, Sengstock C, Groß-Heitfeld C. Silver nanoparticles with different size and shape: equal cytotoxicity, but different antibacterial effects. *RSC Adv*. 2016;6:18490–18501. doi:10.1039/C5RA27836H
29. Inkielewicz-Stepniak I, Santos-Martinez MJ, Medina C, Radomski MW. Pharmacological and toxicological effects of co-exposure of human gingival fibroblasts to silver nanoparticles and sodium fluoride. *Int J Nanomedicine*. 2014;2(9):1677–1687.
30. Peng Y, Song C, Yang C, Guo Q. Low molecular weight chitosan-coated silver nanoparticles are effective for the treatment of MRSA-infected wounds. *Int J Nanomedicine*. 2017;12:295–304. doi:10.2147/IJN.S122357
31. López I.A., Ceballos M., Hernández G., Acosta L., Gómez I., Shape transformation from silver triangular nanoprisms to nanodisks: Raman characterization and sculpturing mechanism. *Revista Mexicana de Fisica*. 2015;61(2):77–82.
32. Suk JS, Xu Q, Kim N, Hanes J, Ensign LM, PEGylation as a strategy for improving nanoparticle-based drug and gene delivery. *Adv Drug Deliv Rev*. 2016;99:28–51. doi:10.1016/j.addr.2015.09.012
33. Liang C, Shangchun L, Xiaochun G, Ping X, Jun C. The role of GSH in microcystin-induced apoptosis in rat liver: involvement of oxidative stress and NF-κB. *Environ Toxicol*. 2016;31(5):552–560.
34. Li H, Cui Z, Han C. Glutathione-stabilized silver nanoparticles as colorimetric sensor for Ni²⁺ ion. *Sensor Actuat B-Chem*. 2009;143(1):87–92. doi:10.1016/j.snb.2009.09.013
35. Silvan JM, Zorruguin-Pena I, Gonzalez de Llano D, Moreno-Arribas MV, Martinez-Rodriguez AJ. Antibacterial activity of glutathione-stabilized silver nanoparticles against *Campylobacter* multidrug – resistant strains. *Front Microbiol*. 2018;9:458. doi:10.3389/fmicb.2018.00458
36. Zabielska-Koczywas K, Dolka I, Król M, et al. Doxorubicin conjugated to glutathione stabilized gold nanoparticles (Au-GSH-Dox) as an effective therapeutic agent for feline injection-site Sarcomas-chick embryo chorioallantoic membrane study. *Molecules*. 2017;22(2):253. doi:10.3390/molecules22020253
37. Turcu I, Zarafu I, Popa M, et al. Lipoic acid gold nanoparticles functionalized with organic compounds as bioactive materials. *Nanomaterials*. 2017;7(2):43. doi:10.3390/nano7120458
38. Kim YS, Kim JS, Cho HS, et al. Twenty-eight day oral toxicity, genotoxicity, and gender-related tissue distribution of silver nanoparticles in sprague-dawley rats. *Inhal Toxicol*. 2008;20:575–583. doi:10.1080/08958370701861512
39. Shrivastava S, Bera T, Singh SK, Singh G, Ramachandrarao P, Dash D. Characterization of antiplatelet properties of silver nanoparticles. *ACS Nano*. 2009;3(6):1357–1364. doi:10.1021/nn900784f
40. Krishnaraj RN, Berchmans S. In vitro antiplatelet activity of silver nanoparticles synthesized using the microorganism *Gluconobacter roseus*: an AFM-based study. *RSC Adv*. 2013;3:8953–8959. doi:10.1039/c3ra41246f
41. Tomaszewski KA, Radomski MW, Santos-Martinez MJ. Nanodiagnosics, nanopharmacology and nanotoxicology of platelet-vessel wall interactions. *Nanomedicine (Lond)*. 2015;10(9):1451–1475. doi:10.2217/nnm.14.86
42. Radomski A, Jurasz P, Sander EJ, et al. Identification, regulation and role of tissue inhibitor of metalloproteinases-4 (TIMP-4) in human platelets. *Br J Pharmacol*. 2002;137(8):1330–1338. doi:10.1038/sj.bjp.0704840
43. Zia F, Kendall M, Watson SP, Mendes PM. Platelet aggregation induced by polystyrene and platinum nanoparticles is dependent on surface area. *RSC Adv*. 2018;8(66):37789–37794. doi:10.1039/C8RA07315E
44. Radomski A, Jurasz P, Alonso-Escolano DA, et al. Nanoparticle-induced platelet aggregation and vascular thrombosis. *Br J Pharmacol*. 2005;146(6):882–893. doi:10.1038/sj.bjp.0706333
45. Dobrovolskaia MA, Patri AK, SImak J, et al. Nanoparticle size and surface charge determine effects of PAMAM dendrimers on human platelets in vitro. *Mol Pharm*. 2012;9(3):382–3923. doi:10.1021/mp200463e

46. Frohlich E. Action of nanoparticles on platelet activation and plasmatic coagulation. *Curr Med Chem.* 2016;23(5):408–430. doi:10.2174/0929867323666160106151428
47. Grant RA, Zucker MB. EDTA-induced increase in surface charge associated with the loss of aggregability. Assessment by partition in aqueous two-phase polymer systems and electrophoretic mobility. *Blood.* 1978;52:515–523.
48. Kälvegren H, Jönsson S, Jonasson L. Release of matrix metalloproteinases-1 and -2, but not -9, from activated platelets measured by enzyme-linked immunosorbent assay. *Platelets.* 2011;22(8):572–578. doi:10.3109/09537104.2011.583300
49. Gresele P, Falcinelli E, Loffredo F, et al. Platelets release matrix metalloproteinase-2 in the coronary circulation of patients with acute coronary syndromes: possible role in sustained platelet activation. *Eur Heart J.* 2011;32(3):316–325. doi:10.1093/eurheartj/ehq390
50. Momi S, Falcinelli E, Giannini S, et al. Loss of matrix metalloproteinase 2 in platelets reduces arterial thrombosis in vivo. *J Exp Med.* 2009;206(11):2365–2379. doi:10.1084/jem.20090687
51. Galt SW, Lindemann S, Allen L. Outside-in signals delivered by matrix metalloproteinase-1 regulate platelet function. *Circ Res.* 2002;90(10):1093–1099. doi:10.1161/01.res.0000022879.57270.11
52. Kuliczowski W, Radoski M, Gąsior M, et al. MMP-2, MMP-9, and TIMP-4 and response to aspirin in diabetic and nondiabetic patients with stable coronary artery disease: a pilot study. *Biomed Res Int.* 2017;2017:9352015. doi:10.1155/2017/9352015
53. Falcinelli E, Giannini S, Boschetti E, Gresele P. Platelets release active matrix metalloproteinase-2 in vivo in humans at a site of vascular injury: lack of inhibition by aspirin. *Br J Haematol.* 2007;138(2):221–230. doi:10.1111/j.1365-2141.2007.06635.x
54. Hosseinzadegan H, Tafti D. Mechanisms of platelet activation, adhesion and aggregation. *Thromb Haemost Res.* 2017;1(2):1008.
55. Espinosa EVP, Murad JP, Khasawneh FT. Aspirin: pharmacology and clinical applications. *Thrombosis.* 2012;2012:173124.
56. Choi WS, Jeon OH, Kim HH, Kim DS. MMP-2 regulates human platelet activation by interacting with integrin α IIb β 3. *J Thromb Haemost.* 2008;6(3):517–523. doi:10.1111/j.1538-7836.2007.02871.x
57. Sang QX, Jin Y, Newcomer RG, et al. Matrix metalloproteinase inhibitors as prospective agents for the prevention and treatment of cardiovascular and neoplastic diseases. *Curr Top Med Chem.* 2006;6(4):289–316. doi:10.2174/156802606776287045
58. Estevez B, Shen B, Du X. Targeting integrin and integrin signaling in treating thrombosis. *Arterioscler Thromb Vasc Biol.* 2015;35(1):24–29. doi:10.1161/ATVBAHA.114.303411
59. Stang K, Krajewski S, Neumann B, et al. Hemocompatibility testing according to ISO 10993-4: discrimination between pyrogen- and device-induced hemostatic activation. *Mater Sci Eng C Mater Biol Appl.* 2014;42:422–428. doi:10.1016/j.msec.2014.05.070
60. Fang W, Chi Z, Li W, Zhang X, Zhang Q. Comparative study on the toxic mechanisms of medical nanosilver and silver ions on the antioxidant system of erythrocytes: from the aspects of antioxidant enzyme activities and molecular interaction mechanisms. *J Nanobiotechnology.* 2019;17:66. doi:10.1186/s12951-019-0502-2
61. Muller L, Steiner SK, Rodriguez-Lorenzo L, Petri-Fink A, Rothen-Rutishauser B, Latzin P. Exposure to silver nanoparticles affects viability and function of natural killer cells, mostly via the release of ions. *Cell Biol Toxicol.* 2018;34:167–176. doi:10.1007/s10565-017-9403-z
62. Wojnicki M, Luty-Błocho M, Kotańska M, et al. Novel and effective synthesis protocol of AgNps functionalized using L-cysteine as a potential drug carrier. *Naunyn Schmiedebergers Arch Pharmacol.* 2018;391(2):123–130. doi:10.1007/s00210-017-1440-x
63. Ferrer MCC, Eckmann UN, Composto RJ, Eckmann DM. Hemocompatibility and biocompatibility of antibacterial biomimetic hybrid films. *Toxicol Appl Pharmacol.* 2013;272(3):703–712. doi:10.1016/j.taap.2013.07.023
64. Huang H, Lai W, Cui M, et al. An evaluation of blood compatibility of silver nanoparticles. *Sci Rep.* 2016;6:25518. doi:10.1038/srep25518
65. Mirshafiee V, Jiang W, Sun B, Wang X, Xia T. Facilitating translational nanomedicine via predictive safety assessment. *Mol Ther.* 2017;25(7):1522–1530. doi:10.1016/j.ymthe.2016.10.004

International Journal of Nanomedicine

Publish your work in this journal

The International Journal of Nanomedicine is an international, peer-reviewed journal focusing on the application of nanotechnology in diagnostics, therapeutics, and drug delivery systems throughout the biomedical field. This journal is indexed on PubMed Central, MedLine, CAS, SciSearch®, Current Contents®/Clinical Medicine,

Journal Citation Reports/Science Edition, EMBase, Scopus and the Elsevier Bibliographic databases. The manuscript management system is completely online and includes a very quick and fair peer-review system, which is all easy to use. Visit <http://www.dovepress.com/testimonials.php> to read real quotes from published authors.

Submit your manuscript here: <https://www.dovepress.com/international-journal-of-nanomedicine-journal>

Dovepress